0 0 0 0 4 7 1 0 3 9 9

UC-34a
UC-25

Submitted to Journal of Chemical Physics

LBL-6220
Preprint

# RADIATION DAMAGE STUDIES BY X-RAY PHOTOELECTRON SPECTROSCOPY I. ELECTRON IRRADIATED $LiNO_3$ AND $Li_2SO_4$

RECEIVED
LAWRENCE
BERKELEY LABORATORY

DEC 15 1977

LIBRARY AND
DOCUMENTS SECTION

T. Sasaki, R. S. Williams,
J. S. Wong, and D. A. Shirley

April 1977

Prepared for the U. S. Department of Energy
under Contract W-7405-ENG-48

For Reference

Not to be taken from this room

LAWRENCE BERKELEY LABORATORY
UNIVERSITY OF CALIFORNIA
BERKELEY

LBL-6220

## DISCLAIMER

This document was prepared as an account of work sponsored by the United States Government. While this document is believed to contain correct information, neither the United States Government nor any agency thereof, nor the Regents of the University of California, nor any of their employees, makes any warranty, express or implied, or assumes any legal responsibility for the accuracy, completeness, or usefulness of any information, apparatus, product, or process disclosed, or represents that its use would not infringe privately owned rights. Reference herein to any specific commercial product, process, or service by its trade name, trademark, manufacturer, or otherwise, does not necessarily constitute or imply its endorsement, recommendation, or favoring by the United States Government or any agency thereof, or the Regents of the University of California. The views and opinions of authors expressed herein do not necessarily state or reflect those of the United States Government or any agency thereof or the Regents of the University of California.

# Radiation Damage Studies by X-ray Photolelectron Spectroscopy
## I. Electron irradiated $LiNO_3$ and $Li_2SO_4$*

T. Sasaki,† R. S. Williams, J. S. Wong, and D. A. Shirley

Materials and Molecular Research Division
Lawrence Berkeley Laboratory
and
Department of Chemistry
University of California
Berkeley, California 94720

April 1977

## ABSTRACT

X-ray photoelectron spectroscopy (XPS) was applied to the study of radiation damage on the surfaces of $LiNO_3$ and $Li_2SO_4$ single crystals which were free of carbon contamination. Irradiations were done in situ at room temperature with 0.3 - 1.6 keV electrons. The products, assigned from chemical shifts in the binding energies of core levels, were: $LiNO_2$ and $Li_2O$ from irradiated $LiNO_3$; and $Li_2SO_3$, elemental sulfur, $Li_2S$, $Li_2O$, and adsorbed oxygen species from irradiated $Li_2SO_4$, respectively. There was no indication in either sample of the metallic lithium formation reported previously. Heavy irradiations of the $Li_2SO_4$ sample showed that the final products of the radiation decomposition are $Li_2O$ and $Li_2S$. The G-values (the number of molecules produced or decomposed per 100 eV of radiation absorbed) of the radiation decomposition and product formation for 1.4 keV incident electrons were estimated from differential energy loss to be approximately $10^{-3}$ - $10^{-4}$.

# I. INTRODUCTION

The nature of radiation damage in crystalline oxyanions has attracted a great deal of attention. In the early 1960's, G. E. Boyd and co-workers did intensive research to determine the products in various alkali-metal bromates exposed to $^{60}Co$ gamma-rays[1] and reactor radiations.[2] Their samples were dissolved and chemical separations were performed on the aqueous solutions. This work yielded much interesting information about molecular products and decomposition mechanisms. However, it is very difficult to elucidate primary stages of reaction mechanisms for radiation decomposition from such studies, because intermediates such as radical species, which coexist with molecular species in the crystal, are not usually stable in the aqueous solution. Recently, Raman spectroscopy combined with optical absorption spectroscopy has proved to be a useful technique for the detection of both ozonide ion $O_3^-$ and molecular oxygen in alkali-metal chlorates irradiated with gamma-rays.[3] Unfortunately this technique cannot be used for detection of the central atom, for which chemical changes provide the most important information about the radiation damage of oxyanions. ESR is a major method for the study of radiation damage in irradiated oxyanions,[4-6] despite the fact that this method cannot detect molecular species, which are often more abundant than radical species in irradiated crystalline solids.

In spite of the promise of the XPS technique, only a few preliminary applications have been made to the radiation damage studies of oxyanions. B. A. De Angelis[7] found radiation-induced reduction of

Cr(VI) to Cr(III) on $CrO_3$ and $K_2CrO_4$ surfaces during XPS measurements. The decomposition of $NaClO_2$, yielding $ClO_3^-$ and $Cl^-$, and of $Li_2S_2O_3$, yielding $SO_3^-$ and elemental sulfur, has also been observed after extended exposure to Al $K_\alpha$ x-rays.[8] From these results, additional product alkali-metal ion lines might also be expected corresponding to the known positions of these lines in the salts that are postulated as decomposition products. However, instead of the Li(1s) lines from such products as LiCl, $Li_2SO_3$, etc., Povey and Sherwood[9] reported observing only the Li(1s) lines from lithium metal and lithium oxide in $LiClO_4$ and $Li_2SO_4$ exposed to source x-rays. For a comprehensive understanding, chemical shifts in binding energies of all the constitutents relevant to the radiation decomposition should be examined.

Radiation damage studies by XPS are of some general importance both intrinsically and because of the detrimental effects of XPS measurements on samples unstable to the source x-rays. The main advantage of this method is that it can in principle provide useful information about molecular products as well as radical species from their chemical shifts. Also, the chemical fate of the alkali-metal ions, which have been neglected in previous radiation damage studies by other methods, can be elucidated.

In the application of XPS to this series of radiation damage studies, the following points were especially taken into consideration: (1) The spectrometer should be designed to detect a given chemical shift with good energy resolution. Monochromatization of the x-rays is desirable. (2) The XPS measurement should be done under UHV conditions to minimize surface contamination with hydrocarbons, oxygen,

water vapor, etc. (3) Low-energy electrons or ions should be employed as a radiation source because they produce damage on the sample surface far more efficiently than soft x-rays in a photoelectron spectrometer. (4) In situ irradiation under high-vacuum conditions is indispensable for the prevention of chemical reactions between the products and their surroundings.

In this paper, the observation of radiation decomposition on the surfaces of $LiNO_3$ and $Li_2SO_4$ single crystals following electron irradiations is described and a useful approach to the study of radiation damage using XPS is presented.

## II. EXPERIMENTAL

Lithium salts were used in the present study, because the Li(1s) line which falls at ca. 56 eV binding energy does not hinder the examination of changes in the valence band spectra of the nitrate and sulfate ions. The single crystals of $LiNO_3$ and $\alpha$-$Li_2SO_4$ were prepared from their melts. The A.R. grade $LiNO_3$ and $Li_2SO_4 \cdot H_2O$ were each heated slowly in Pt crucibles to 300°C and 900°C, respectively, and the melts were cooled at 80°C/day. The highly hygroscopic single crystals so obtained were kept in a vacuum desiccator until the XPS measurements. Before mounting in sample holders, the cleaved samples were annealed at 200°C for 2 hours in air. This pre-treatment was judged to be useful for elimination of active sites for carbon contamination because no carbon was found on the sample surfaces after the duration of the experiment (ca. 7 days). After cooling, the crystals were scraped or cleaved again in a glove bag filled with dry nitrogen, and placed in sample holders which

were mounted immediately in the spectrometer.

High-resolution XPS measurements were carried out with a Hewlett-Packard 5950A ESCA Spectrometer employing monochromatized Al Kα x-rays (1486.6 eV) at pressures less than $1 \times 10^{-9}$ Torr. To minimize the effect of surface charging on the peak width, the sample surface was flooded with low-energy electrons. The optimum conditions of the flood gun were determined to be 0.8 mA and 2 V for $LiNO_3$ and 0.6 mA and 2 V for $Li_2SO_4$, respectively. Usually the first run was a 0 - 1280 eV overall scan to check sample contamination. Several narrow scans of core-level peaks were then taken, and finally a valence band spectrum was taken. After long-term measurements of the valence region, which took about 17 hours, no radiation damage by the Al Kα x-rays was observed.

Irradiations were done at room temperature in the preparation chamber with 0.3 - 1.6 keV electrons from an electron gun source. The schematics of the experimental set-up for the $Li_2SO_4$ specimen are shown in Fig. 1. For this geometry direct heat from the filament was estimated to be negligible at the sample position. The electron energy and filament current, normally 1 mA, were monitored and adjusted to be constant during the irradiation. To determine the absolute current at the sample position, the sample was replaced with a shielded, stainless-steel Faraday cup whose inlet dimensions were the same as those of the sample surface (5mm x 7mm). After the irradiation, during which the pressure remained less than $4 \times 10^{-8}$ Torr, the sample was re-introduced into the analyzer chamber for XPS measurement. Neither broadening nor energy shifts of the core-level peaks caused by irradiation were observed.

Binding energies were determined relative to the Fermi levels of the respective solids. The published valence band spectra[8,10] also served as references for binding energies and molecular orbitals observed in the present work. Relative product yields were estimated from the areas of the respective peaks by integrating with a planimeter. In the case of the O(1s) line from the irradiated samples, the spectra were unfolded by computer analysis into several Gaussian components whose half-widths were taken from the O(1s) line of the unirradiated samples.

## III. RESULTS AND DISCUSSION

### A. Product Assignments in Irradiated $LiNO_3$

The $LiNO_3$ sample was irradiated with 1 keV electrons. A two-hour irradiation at 1 mA filament current did not change the color of the sample surface. Figure 2 shows a spectral change in the N(1s) region of the XPS spectrum. The total current density is indicated by $I_c$, in units of $10^{-1}$ Coulomb/cm$^2$. Figure 2(a) and Fig. 2(b) are spectra before and after the electron irradiation, respectively, and are normalized to the intensity of the parent $LiNO_3$. Irradiation causes the appearance of peak A, with a binding energy lower by 3.6 eV than that of the parent. The product was so stable chemically that further radiation decomposition was not observed upon continued irradiation. Since the position of the N(1s) product peak did not change with total radiation dose, the chemical form of the product can be inferred from its chemical shift. By comparison with the -3.3 eV shift in the N(1s) energy of $NaNO_2$ from that of $NaNO_3$ observed by Hollander et al.,[11] the observed product is probably $NO_2^-$. This is consistent with the generally-agreed overall reaction in crystalline nitrates irradiated at room temperature:[12]

$$MNO_3 \rightarrow MNO_2 + 1/2\ O_2 \quad .$$

Because only one nitrogen-containing product was observed, peak A cannot be associated with such radicals as $NO_2$ and/or $NO_3$, to which a weak ESR signal observed for room temperature irradiated $NaNO_3$ was tentatively assigned.[13] The N(1s) lines from such radicals should be well-resolved from the two observed lines.

Figure 3 presents the spectral changes in the O(1s) region. The broken lines in Fig. 3(b) were obtained by computer deconvolution in which three Gaussians were employed. There are two new peaks, B and C. Because the presence of $NO_2^-$ has been confirmed in Fig. 2, the appearance of the O(1s) line from the same ion is expected. Based on an empirical curve for the O(1s) chemical shifts on various compounds given by Nefedov et al.,[14] we can estimate the O(1s) energy of $NO_2^-$ (perhaps present as $LiNO_2$) to be 1.7 eV lower than that of $NO_3^-$, assuming atomic distances R(O - Li) and R(O - N) are 1.0 Å[15] and 1.13 Å,[16] respectively. Therefore peak B, with binding energy 1.85 eV less than that of the parent, is attributed to $NO_2^-$. This assignment is also supported by a quantitative analysis of the product yield. Computer deconvolution showed that the O(1s) intensity of $NO_2^-$ relative to the parent is 0.44, while the relative N(1s) intensity of $NO_2^-$ is 0.64. The correction by stoichiometry yields 0.66 (=0.44 x 3/2) for the latter, which agrees very well with the $NO_2^-$ product yield from the N(1s) intensity. On the other hand peak C, which is located at a position lower by 4.6 eV than the parent, arises from one of the products ubiquitous on the surfaces of irradiated lithium oxyanion salts. We assign this to an O(1s) peak from $Li_2O$. A chemical shift of -3.8 eV from the parent is estimated from the empirical curve given for the O(1s) energy with the value of 1/R appropriate for $Li_2O$.[14] This shift is fairly large

for oxygen in the -2 oxidation state, but the O(1s) energies of the alkali-metal oxides are known to be generally lower than those of other alkali-metal compounds containing oxygen.[17] Such large shifts are due to the especially strong polarization effects of $Li^+$. There was no indication of $O^-$ or $O_2^-$, the formation of which has been confirmed for gamma-irradiated $NaNO_3$.[18]

A gradual shift in the Li(1s) line to lower binding energy with irradiation time was also observed. It amounted to 2.7 eV for a radiation exposure of 0.051 Coulomb/$cm^2$. The new Li(1s) line had a smaller shoulder on the higher binding energy side. The chemical shift we observe is less than the value reported by Povey and Sherwood,[9] who observed a chemical shift of ca. 4.8 eV for the Li(1s) energy of $Li_2O$ in $LiNO_3$ powder exposed to source x-rays. We note that the product peak is due to $Li_2O$ mixed with $LiNO_3$ and $LiNO_2$. Povey and Sherwood also reported metallic lithium formation on the $LiNO_3$ sample. However, in the present study, no Li(1s) peak attributable to metallic lithium was observed. In a related experiment, we observed radiation decomposition of $LiClO_4$ exposed to Al $K_\alpha$ x-rays. The spectral changes in the valence band, Cl(2p), and Li(1s) regions showed formation of $LiClO_3$ as a major product containing $Li^+$, but there was no indication of lithium metal formation. Although formations of colloidal metal particles by low-energy (500 eV)[19] and high-energy (3.5 MeV)[20] electron irradiations of alkali halides have been observed, metal formation is not as well-characterized for irradiated oxyanion salts. The metallic yields determined by Povey and Sherwood[9] were less than 5% of the total intensity of the Li(1s) line and depended upon sample preparation. In our studies there was no major difference in the

valence band spectra before and after electron irradiation because of the similarity in the molecular-orbital energy levels of $LiNO_2$ and $LiNO_3$. The only difference of note is the appearance of a new peak around 22 eV which is the O(2s) line of $Li_2O$.

B. Product Assignments in Irradiated $Li_2SO_4$

The sample surface showed a gradual black coloration which increased with irradiation time and was insensitive to photobleaching. Figure 4 shows the spectral change in the S(2p) region. The absolute total intensity decreased with irradiation time and the relative S(2p) intensities in Figs. 4(b) and 4(c) were 0.84 and 0.58 times that in Fig. 4(a), respectively. After electron irradiation, the S(2p) line split into peaks attributable to three different chemical forms, labeled D, E, and F. As the effect of the chemical mixture on binding energy is negligibly small, the chemical forms of the products may be determined from the spectrum as in the case of $LiNO_3$ radiation products. The S(2p) energies and the chemical shifts of the products are given in Table I. Extensive work has been done on the chemical shifts of sulfur compounds.[21-24] Theoretical considerations lead to correlations between the chemical shift and the atomic charge which can be obtained from simple quantum-chemical calculations or more simply from Pauling's empirical equation for partial ionic character of the chemical bond. Comparisons of the present chemical shifts with the published data for the S(2p) binding energy yield the oxidation states of the sulfur products. The chemical shifts for the S(2p) energies of some related compounds are listed in Table II, and the chemical forms of the products are identified as shown in brackets in the first column of Table I.

Figure 5 shows the spectral change in the O(1s) region. The irradiation causes a decrease in the absolute O(1s) intensity as in the case of the S(2p) line. Deconvolution of Fig. 5(b) indicates there appear to be at least four products (G, H, I, and J) containing chemically different oxygen, as displayed in Fig. 6. The most intense peak is the O(1s) line from the parent $SO_4^{2-}$. Peak G is assigned as oxygen trapped or more likely adsorbed strongly on the surface layer, because it showed a dependence on pressure during electron irradiation. It is well known that the O(1s) spectrum of oxygen chemisorbed on metals and oxides does not show a detectable multiplet splitting,[25] which is clearly observed for gaseous molecular oxygen.[26] Furthermore, the electronic environment of chemisorbed oxygen is quite different from that of gaseous oxygen (its O(1s) energy is lowered by as much as 13 eV compared with that of gaseous state[25]). Correct assignment of product H requires further examination, but such species as $O_2^-$ and $O_3^-$ trapped in the surface layer are considered as possible forms on the grounds that the oxygen in the product H should be in an oxidation state between 0 and -2. In addition, $O_3^-$ is usually found in irradiated oxyanions such as $Na_2SO_4$[5] at room temperature, and is stable up to 150°C in gamma-irradiated $K_2SO_4$.[6] Peak I can be attributed to $SO_3^{2-}$, because the intensity relative to that of the parent, after stoichiometric correction, is nearly equal to the corresponding intensity ratio determined for the S(2p) peak in Fig. 4. A small chemical shift for the O(1s) energy between $SO_4^{2-}$ and $SO_3^{2-}$ has also been observed elsewhere.[21,22] Peak J, corresponding to a highly polarized form, becomes increasingly intense with irradiation time and seems to be the final oxygen-containing product. It is assigned as the O(1s) peak from $Li_2O$,

which is also present in irradiated $LiNO_3$ and $LiClO_4$. A calculation based on Nefedov's empirical curve[14] showed that the expected chemical shift from the parent is -1.9 eV, while a -3.0 eV shift is obtained from Fig. 6.

Any analysis of an unresolved peak into components is subject to doubt, and this interpretation must be regarded in that context. It is clear by visual inspection of Fig. 6 that at least five simple lines are needed to fit the spectrum. More could be used of course, and the intensity ratios are not unique. Thus our interpretation is only the most plausible we can offer. A disturbing feature of this spectrum is the shift of the main O(1s) peak by nearly 1 eV on irradiation. This can be rationalized in terms of the reducing environment, but is not really explained.

Spectral changes in the valence band region, including the Li(1s) line, are shown in Fig. 7. These spectra do not give any definite evidence for the formation of $SO_3^{2-}$ because it has a valence band spectrum very similar to that of the parent.[8] Irradiation causes a gradual decrease in the absolute intensity of the valence band spectrum, and new peaks (I) and (II) appear at 22 and 6 eV. These are the O(2s) and O(2p) lines from $Li_2O$, adsorbed oxygen, etc. The distortion of peak (II) may be due to a small contribution from the S(3p) line. The photoionization cross-section of S(3p) at Al $K_\alpha$ energies is estimated to be small, but larger than that of the S(3s) shell.[27] A small change in the Li(1s) line is also seen in Fig. 7 with a chemical shift of -1.4 eV from the parent. Since there are four possible anions associated with $Li^+$, the chemical shift observed is too small to be assigned unambiguously. We

emphasize again that these spectra do not contain a peak attributable to metallic lithium.

For quantitative analysis, the relative intensities of the S(2p) peaks are plotted against the total current density of the incident electrons in Fig. 8. The initial slopes of these curves will be used in the next section to estimate G-values. In the heavy irradiations, the increasing rate of sulfide yield is far larger than that of the $SO_3^{2-}$ yield, and is slightly larger than the decreasing rate of the parent. This means that sulfide is one of the common radiation products from both $SO_4^{2-}$ and $SO_3^{2-}$. Figure 9 shows growth curves of the oxygen containing products. While the yield of the product G (not G-value, chemical species indicated as G in Fig. 6) decreases in the heavy irradiations, the $SO_3^{2-}$ peak, peak H (possibly absorbed oxygen), and the $Li_2O$ peak yields show no sign of decline. The relative concentrations of $SO_4^{2-}$ and $SO_3^{2-}$ predicted by the intensity profiles of Figs. 8 and 9 agree quite well with one another (within a few percent) when the correction for stoichiometry has been applied to the results of Fig. 9.

## C. Estimation of G-Values

An estimate of the absolute yields of the products is especially important because little is known about the formation of molecular species in solids. For this purpose the G-values should be determined. Because the incident electrons penetrate far beyond the depth detected in XPS measurements, the quantity obtained in this study is different from the G-value usually adopted in radiation chemistry, but it may provide important information about the distribution of products along the

tracks of incident electrons. We shall consider the G-value for radiation decomposition of those parent molecules which lie in the initial layer of thickness equal to the effective sampling depth for photoelectrons originating from S(2p) levels of $Li_2SO_4$ radiation decomposition products. It will be shown that this value can be estimated from the initial slope of the parent concentration curve (Fig. 8), assuming that the sulfur-containing products are only $SO_3^{2-}$, elemental sulfur, and sulfide.

The radiation decomposition product concentration P is defined as

$$P = N_d/N_t \quad , \tag{1}$$

where $N_d$ and $N_t$ are, respectively, the number of molecules radiolitically decomposed and the total number of parent molecules originally in the layer of thickness corresponding to the effective photoelectron sampling depth $\lambda'$. The quantity $N_d$ is related to the G-value for radiation decomposition by

$$N_d = E_{ab}\ G/100 \quad . \tag{2}$$

Here $E_{ab}$ (in eV) is the net energy absorbed per unit surface area in the layer $\lambda'$ due to inelastic collisions. $E_{ab}$ is approximately given by

$$E_{ab} \simeq N_e(E_{e1} - E_{e2}) \quad , \tag{3}$$

where $E_{e1}$ and $E_{e2}$ are the incident electron energy and the average kinetic energy of an electron which has traversed the layer of thickness $\lambda'$. $N_e$, the total number of electrons striking the unit area of the sample surface, is given by $N_e = C \times 6.24 \cdot 10^{18}$, where C is the total incident charge per unit surface area, in units of Coulomb/$cm^{-2}$. From

Eqs. (1) - (3) the G-value is expressed as

$$G \simeq \frac{A \cdot \rho \cdot \lambda'}{M(E_{e1} - E_{e2})} \frac{P}{C} \times 1.6 \times 10^{-17} \quad , \tag{4}$$

where A is Avogadro's number, $\rho$ is the mass density of the target and M the molecular weight. To determine the G-value, $\lambda_e$ (the inelastic collision mean-free path) in $Li_2SO_4$ was evaluated from an equation given by D. R. Penn,[28] and is plotted as a function of the incident electron energy in Fig. 10. The extrapolated penetration range $R_e$ (Fig. 10) of the incident electrons, which is required to estimate $E_{ab}$, was calculated on the basis of a semiempirical equation by T. Tabata, et al.[29] From the geometrical considerations[30] of Fig. 1 and the $\lambda_e$ values, $\lambda'$ is estimated to be 13 Å for S(2p) photoelectrons (K. E. ∿1320 eV) produced by Al Kα x-rays, while $R_e$ of incident 1400 eV electrons is 599 Å. Therefore the average energy $E_{e2}$ corresponds to an electron energy with an $R_e$ value of 586 Å, or 1374 eV. Consequently, ca. 26 eV is lost in the surface layer of thickness $\lambda'$. This estimate is consistent with the production of secondary electrons described below. As the density of $Li_2SO_4$ is 2.22 g/cm$^3$, Eq. (4) is simplified to

$$G \simeq 9.7 \times 10^{-4} \, (\Delta P/\Delta C)_i \quad , \tag{5}$$

where $(\Delta P/\Delta C)_i$ means an initial slope for the decrease of the parent with incident charge in the $\lambda'$ layer. $(\Delta P/\Delta C)_i$ in Eq. (5) is the initial slope for the decrease of $SO_4^{2-}$ in Fig. 8, which is -4.2 (±50%). Therefore, the G-value becomes ca. $-4.1 \times 10^{-3}$, where the negative sign indicates radiation decomposition. In other terms, a 20% decomposition of the surface

layer of a $Li_2SO_4$ crystal requires 1100 of 1.4 KeV electrons per surface sulfate ion. The G-values for the products were also determined from the corresponding slopes, and are listed in the fourth column of Table I.

We must now discuss the severity of the approximations made in the G-value estimates. The sampling depth $\lambda'$ is smaller than the $\lambda_e$ value for the bombarding electrons (22 Å), so the region from which the XPS signal originates is probably uniform (i.e., a homogeneous distribution of radiation products exists within $\lambda'$). The estimate of $E_{e2}$ is probably correct to within 15%,[29] but $E_{ab}$ is also strongly dependent upon the secondary electron spectrum, as secondary electrons may transmit appreciable amounts of energy outside this layer. Energy- and angular-resolved secondary electron spectra have been measured for various gases irradiated with 0.5 - 2.0 keV electrons.[31,32] These measurements showed that most secondary electrons have energies below 70 eV. This is the energy regime in which $\lambda_e$ increases drastically with decreasing electron kinetic energy.[33] Thus, a significant proportion of the energy deposited in the layer $\lambda'$ may be removed by secondary electrons escaping into vacuum, but this energy loss is partly compensated by secondary electrons from deeper within the crystal. Finally, the estimates of the initial radiation decomposition rates from $(\Delta P/\Delta C)_i$ are lower limits due to further decomposition of products. Thus, the G-value calculated for $SO_4^{=}$ decomposition is a lower limit for the actual value.

## IV. CONCLUSION

Although further refinement is necessary, especially for the estimate of the energy deposited in a layer of thickness $\lambda'$, the present analysis

gives a useful approach to quantitative determination of the radiation products in surface layers. In addition, irradiations with incident electron energies lower than 0.3 keV, which were not experimentally feasible in the present study, will provide important information about chemical changes near the terminus of an electron track, where energy transfer becomes quite large.

*Work done under the auspices of the U.S. Energy Research and Development Administration.

+Present address: Chemistry Division, Japan Atomic Energy Research Institute, Tokai-mura, Ibaraki-ken 319-11, Japan.

[1] G.E.Boyd, E.W.Graham, and Q.V.Larson, J. Phys. Chem. 66, 300 (1962).

[2] G.E. Boyd and Q.V. Larson, J. Phys. Chem. 68, 2627 (1964).

[3] J.B. Bates and J.C. Pigg, J. Chem. Phys. 62, 4227 (1975); J.B. Bates and J.C. Pigg, J. Chem. Phys. 65, 3901 (1976).

[4] See, for example, D. Suryanarayana and J. Sobhanadri, J. Magn. Resonance 16, 274 (1974).

[5] N. Hariharan and J. Sobhanadri, Mol. Phys. 17, 507 (1969).

[6] T. Sasaki, Phys. Stat. Sol. (a) 34, 339 (1976).

[7] B.A.De. Angelis, J. Electron Spectrosc. 9, 81 (1976).

[8] R. Prins, J.Chem. Phys. 61, 2580 (1974).

[9] A.F.Povey and P.M.A. Sherwood, J.Chem. Soc. Farad. Trans. II. 70, 1240 (1974).

[10] J.F. Wyatt, I.H. Hillier, V.R. Saunders, J.A. Connor, and M. Barber, J. Chem. Phys. 54, 5311 (1971); M. Barber, J.A. Connor, I.H. Hillier, and V.R. Saunders, in Electron Spectroscopy, edited by D.A. Shirley (North-Holland, Amsterdam, 1972), p. 379; J.A. Connor, I.H. Hillier, V.R. Saunders, and M. Barber, Mol. Phys. 23, 81 (1972); A. Calabrese and R.G. Hayes, J. Electron Spectrosc. 6, 1 (1975); V.I. Nefedov, Y.U. Buslaev, N.P. Sergushin, Y.V. Kokunov, and V.V. Kovalev, J. Electron Spectrosc. 6, 221 (1975).

[11] J.M. Hollander, D.N. Hendrickson, and W.L. Jolly, J. Chem. Phys. 49, 3315 (1968).

[12]E.R. Johnson, The Radiation-Induced Decomposition of Inorganic Molecular Ions (Gordon and Breach, New York, N. Y., 1970) pp. 33-85.

[13]W.B. Ard, Jr., J. Chem. Phys. 23, 1967 (1955); D. Shoemaker and E. Boesman, C. R. Acad. Sci. 252, 2099, 2865 (1961).

[14]V.I. Nefedov, N.P. Sergushin,and Ja. V. Salyn, J. Electron Spectrosc. 8, 81 (1976).

[15]E. Zintl, A. Hader, and B. Dauth, Ztsch. Electrochem. 40, 588 (1934).

[16]R.W.G. Wyckoff, Crystal Structures Vol III(Interscience Publishers, 1960) p. 359.

[17]A. Barrie and F.J. Street, J. Electron Spectrosc. 7, 1 (1975).

[18]A. Frances and E.R. Johnson, J. Phys. Chem. 79, 35 (1975).

[19]L.S.C. Araiza and B.A. Powell, Surf. Sci. 51, 504 (1975).

[20]Y.A. Ekmanis and E.A. Rosauer, J. Appl. Phys. 46, 2837 (1975).

[21]B.J. Lindberg, K. Hamrin, G. Johansson, U. Gelius, A. Fahlman, C.Nordling, and K. Siegbahn, Phys. Scr. 1, 286 (1970).

[22]K. Siegbahn, C.N. Nordling, A. Fahlman, R. Nordberg, K. Hamrin, J. Hedman, G. Johansson, T. Bergmerk, S.E. Karlsson, I. Lindgren, and B. Lindberg, ESCA, Atomic, Molecular and Solid State Structure Studied by Means of Electron Spectroscopy(Almqvist and Wiksells, Uppsala, 1967).

[23]L.N. Kramer and M.P. Klein, Chem. Phys. Lett. 8, 183 (1971).

[24]U. Gelius, B. Roos, and P. Siegbahn, Chem. Phys. Lett. 4, 471 (1970).

[25]G. Schōn and S.T. Lundin, J. Electron Spectrosc. 1, 105 (1972/1973); K.S. Kim and R.E. Davis, J. Electron Spectrosc. 1, 251 (1972/1973); R.W. Joyner and M.W. Roberts, Chem. Phys. Lett. 28, 246 (1974).

[26]J. Hedman, P.-F. Heden, C. Nordling, and K. Siegbahn, Phys. Lett. 29A, 178 (1969); P.S. Bagus, M. Schrenk, D.W. Davis, and D.A. Shirley, Phys. Rev. A9, 1090 (1974).

[27]R.C.G. Leckey, Phys. Rev. A13, 1043 (1976).

[28]D.R. Penn, J. Electron Spectrosc. 9, 29 (1976).

[29]T. Tabata, R. Ito, and S. Okabe, Nucl. Instr. Method 103, 85 (1972).

[30]R.S. Williams, S.P. Kowalczyk, P.S. Wehner, G. Apai, J. Stöhr, and D.A. Shirley, submitted to J. Electron Spectrosc.

[31]C.B. Opal, E.C. Beaty, and W.K. Peterson, At. Data 4, 209 (1972).

[32]Y.-K. Kim, in Proceedings of the Fifth International Congress of Radiation Research, edited by O.F. Nygaard, H. I. Adler, and W.K. Sinclair (Acad. Press, New York, 1975) p. 219

[33]I. Lindau and W.E. Spicer, J. Electron Spectrosc. 3, 409 (1974).

TABLE I. The $S2p_{3/2}$ binding energies and G-values of the products.

| Chemical forms | E(ev) | ΔE(ev) | G (±50%) |
|---|---|---|---|
| $SO_4^{2-}$ | 168.1 | 0 | $-4.1\times10^{-3}$ |
| D ($SO_3^{2-}$) | 165.5 | 2.6 | $3.4\times10^{-3}$ |
| E (elemental) | 162.2 | 5.9 | $8.4\times10^{-5}$ |
| F ($S^{2-}$) | 158.8 | 9.3 | $6.4\times10^{-4}$ |
| Sum of products | | | $4.1\times10^{-3}$ |

TABLE II. The S2p energies of some related compounds and averaged chemical shifts from the $SO_4^{2-}$ peak.

| Compounds | E(eV) | $\Delta E_{av}$(eV) |
|---|---|---|
| $Na_2SO_4$ | 168.9 [a] | |
| | 167.7 [b] | 0 |
| $Na_2SO_3$ | 166.7 [a] | |
| | 165.8 [b] | 2.1 |
| $S_8$ | 164.2 [a] | |
| | 162.2 [b] | 5.1 |
| $Na_2S$ | 162.0 [a] | |
| | 160.8 [b] | 6.9 |

[a] From ref. 21.

[b] From ref. 22.

FIGURE CAPTIONS

Fig. 1. Experimental geometry for (a) electron irradiations and (b) XPS measurements. S: sample, H: sample holder, G: electron gun, A: analyzer system, $\Theta = 38°$, $\phi = 78°$.

Fig. 2. Spectral changes in the N(1s) region of irradiated $LiNO_3$. Peak A is assigned to product $NO_2^-$. $I_c$ is in units of Coulomb/$cm^2$.

Fig. 3. Spectral changes in the O(1s) region of irradiated $LiNO_3$. Peak B is assigned to product $NO_2^-$ and Peak C to product $Li_2O$.

Fig. 4. Spectral changes in the S(2p) region of irradiated $Li_2SO_4$. Each peak is $2p_{1/2}$-$2p_{3/2}$ doublet only partially resolved. Peak D is assigned to product $SO_3^{2-}$, Peak E to elemental sulfur, and Peak F to $S^{2-}$ (see Table I).

Fig. 5. Spectral changes in the O(1s) region of irradiated $Li_2SO_4$. (See Fig. 6 for product assignments.)

Fig. 6. Computer unfolding of the spectrum of Fig. 5(b). The darker line is the sum of five Gaussian components. Peaks G and H may be due to adsorbed oxygen and $O_2^-$ (or $O_3^-$), respectively. Peak I is assigned to product $SO_3^{2-}$ and Peak J to $Li_2O$.

Fig. 7. Spectral changes in the valence band region of irradiated $Li_2SO_4$. In part (a), the molecular orbitals are clearly evident. In part (c), Peak (I) is assigned to O(2s) and Peak (II) to O(2p) associated with the reduced species and $Li_2O$.

Fig. 8. Relative S(2p) intensities of the products on the irradiated $Li_2SO_4$ surface versus total radiation dose.

Fig. 9. Relative O(1s) intensities of the products on the irradiated $Li_2SO_4$ surface versus total radiation dose.

Fig. 10. Calculated inelastic collision mean-free path $\lambda_e$ and extrapolated range $R_e$ of electrons in $Li_2SO_4$ as a function of kinetic energy. Semiempirical equations given by D. R. Penn[28] and T. Tabata, et al.[29] were used for the calculations of $\lambda_e$ and $R_e$, respectively. The dashed extrapolations of these curves reflect the expected behavior for electrons with energies approaching the bottom of the conduction band (for $\lambda_e$, see Ref. 33).

0 0 0 0 4 7 1 0 6 1 2



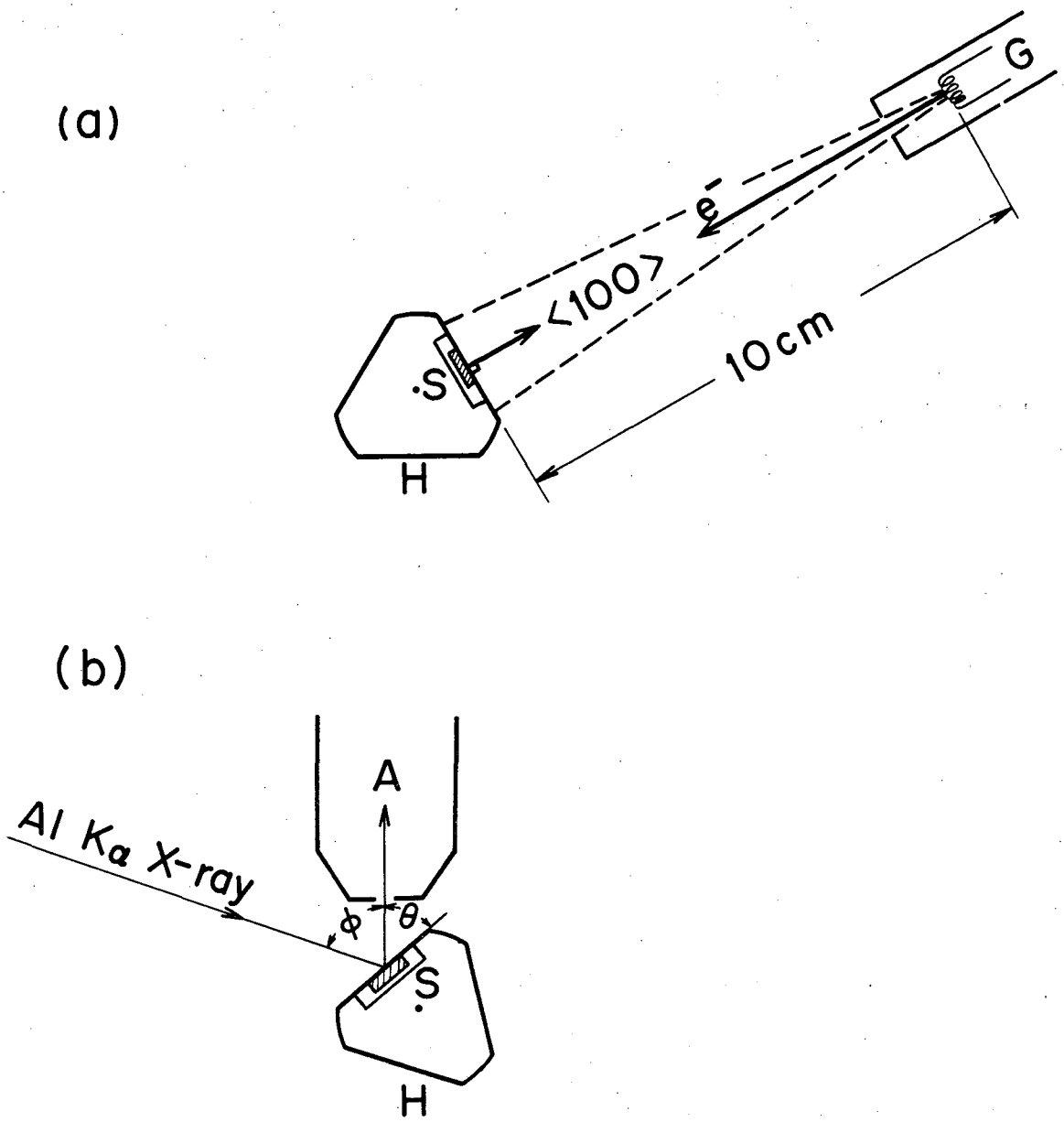


XBL 7710-6844

Fig. 1

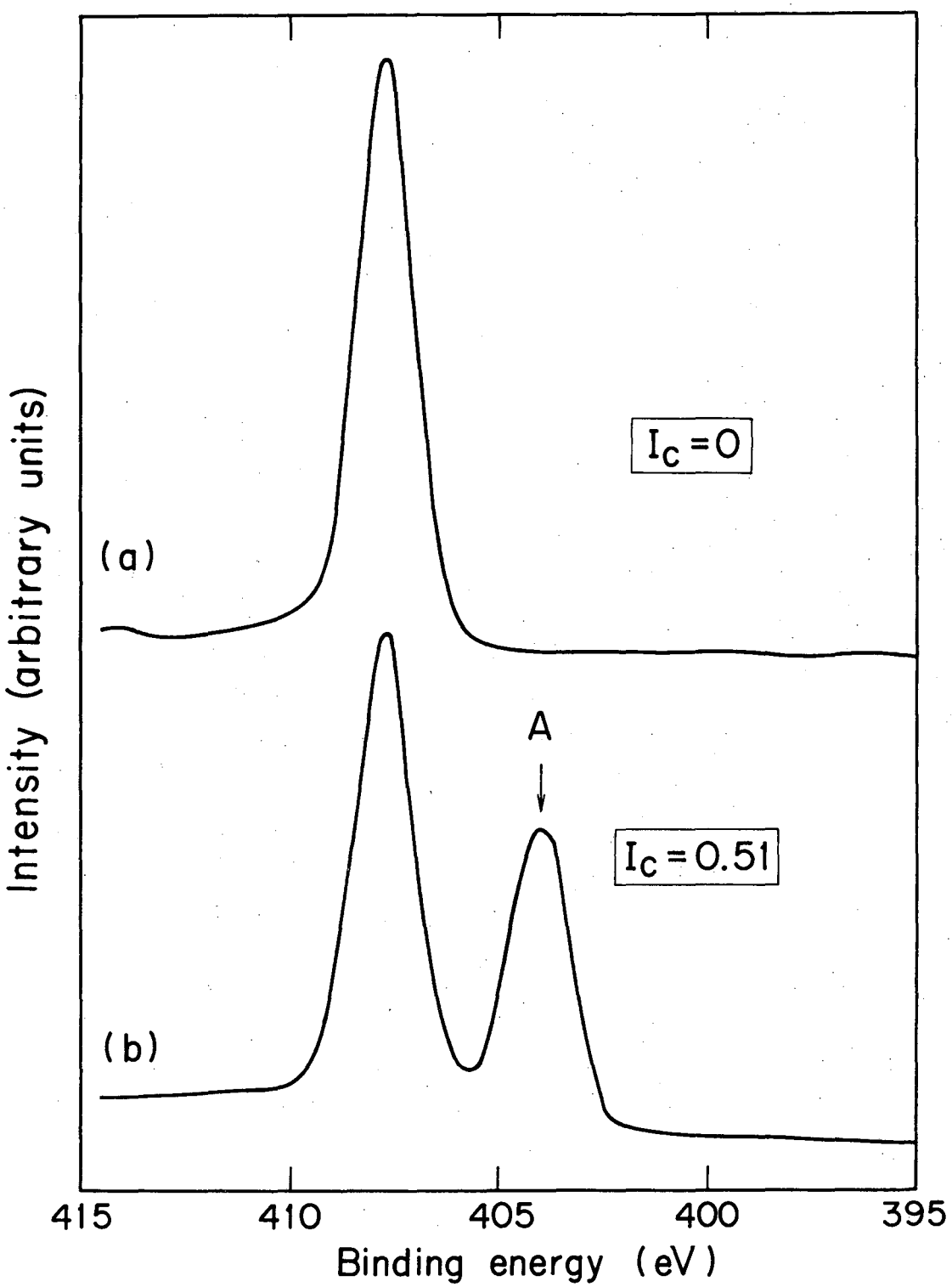


XBL 7710-6852

Fig. 2

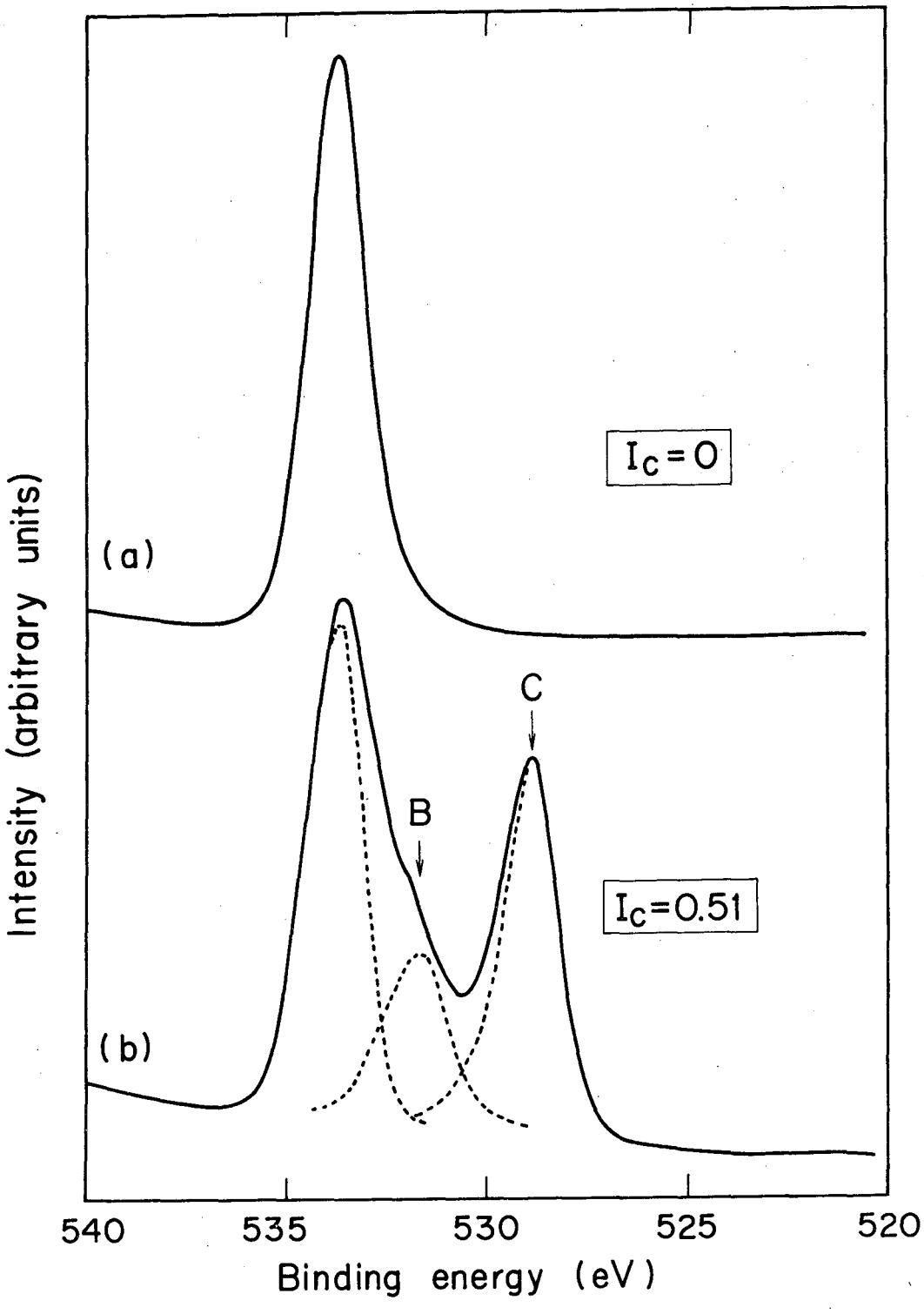


XBL 7710-6851

Fig. 3

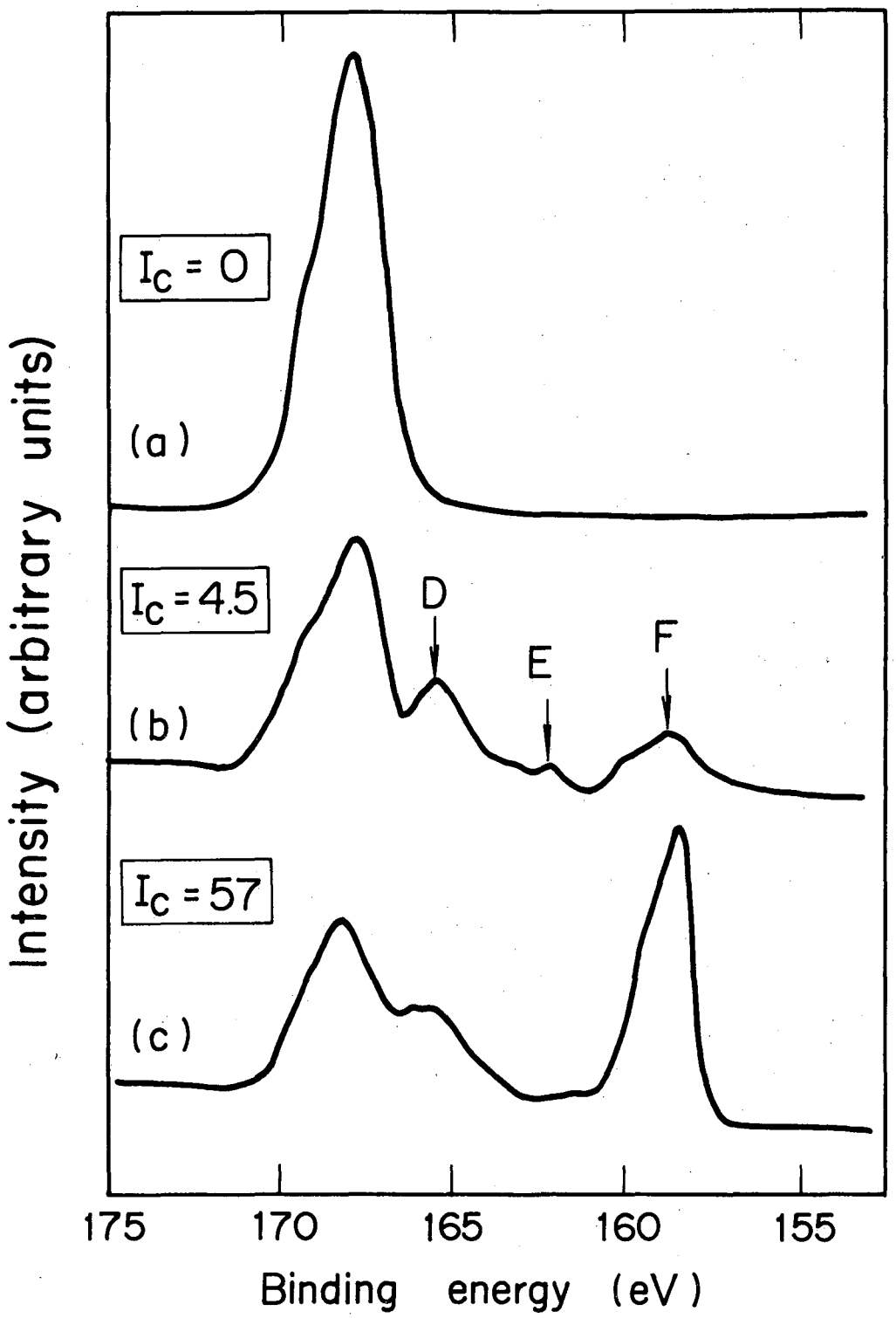


Fig. 4 XBL 7710-6845

0 0 0 0 4 7 1 0 6 1 4



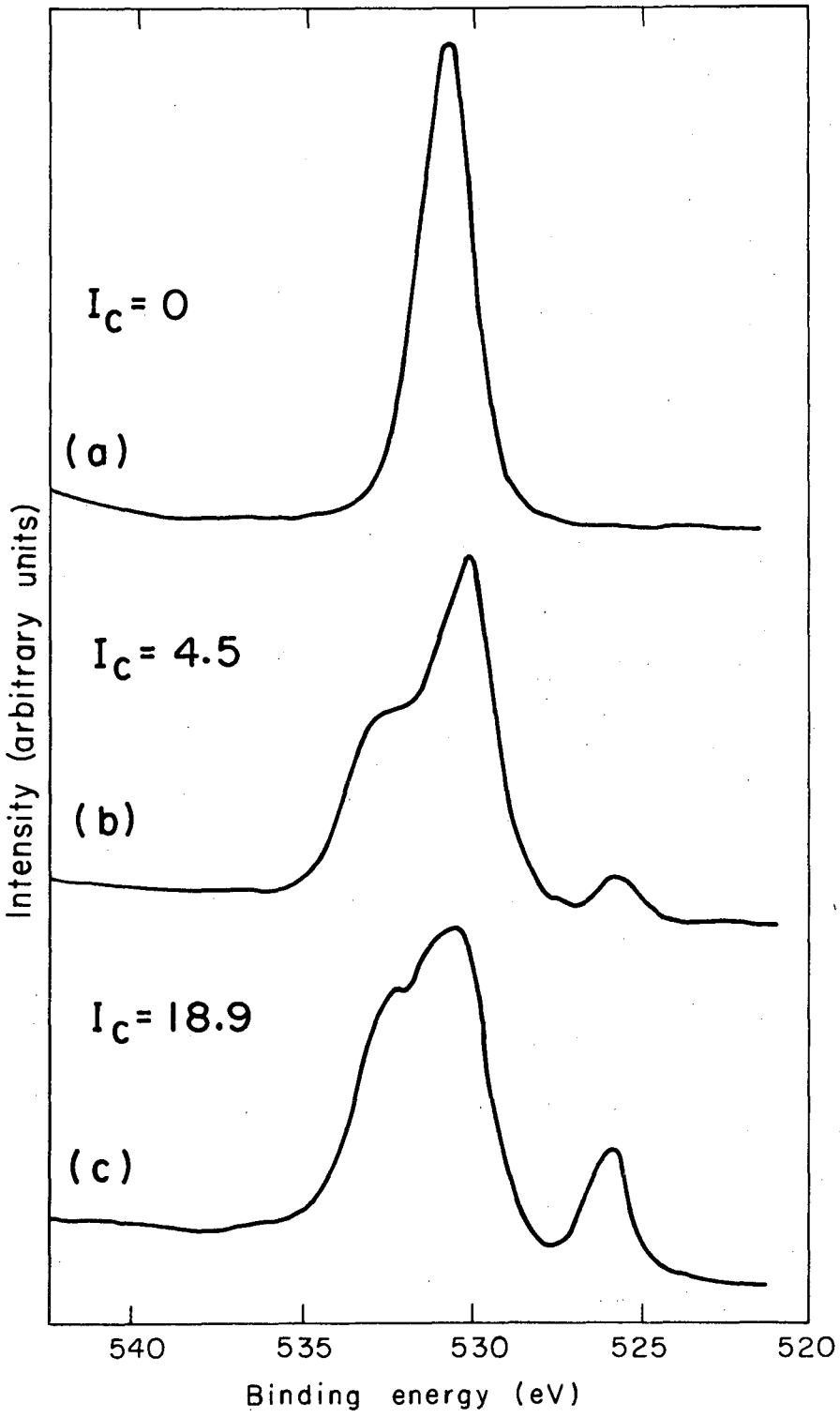


Fig. 5

XBL7612-11149

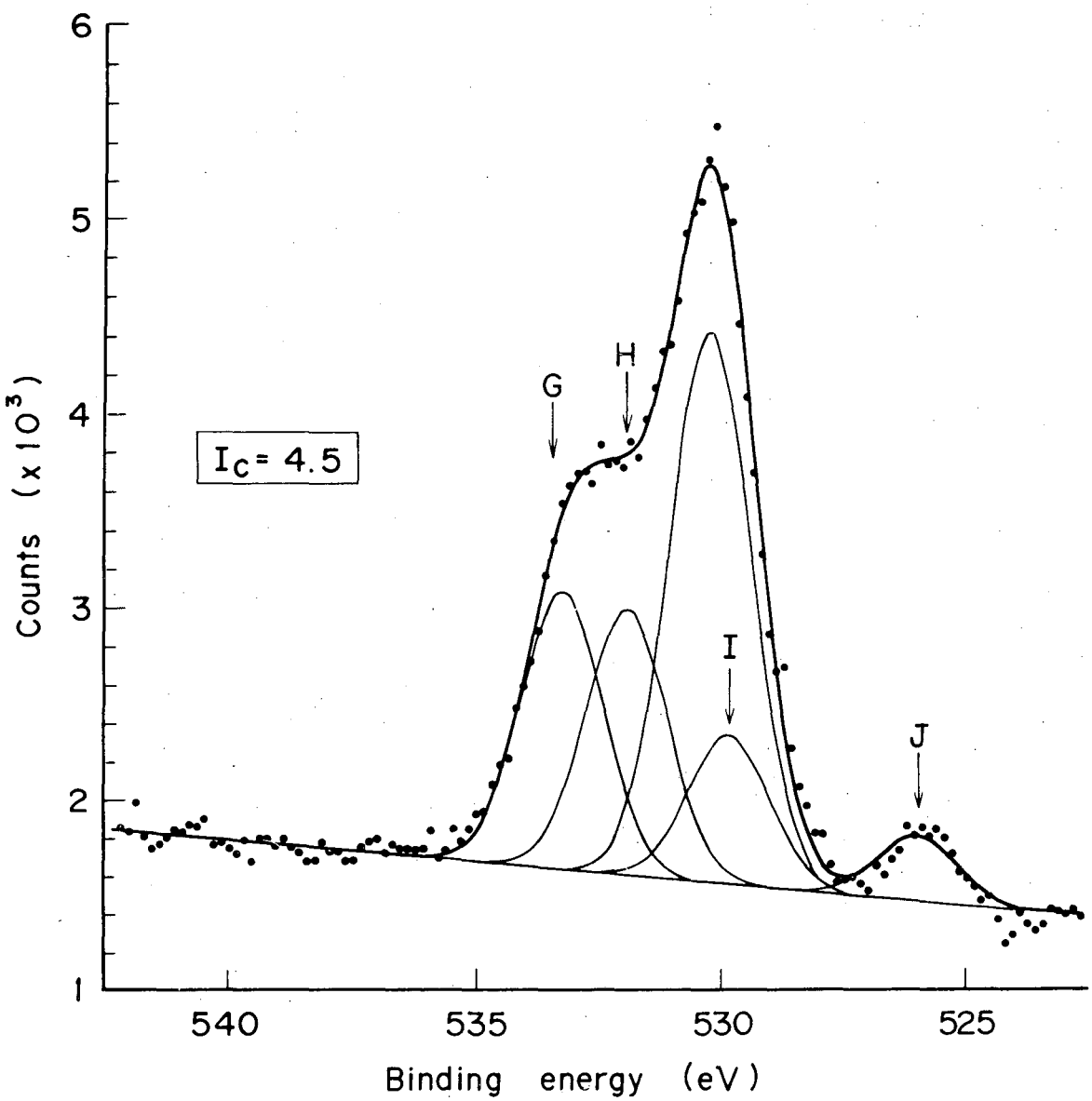


Fig. 6

XBL 7710-6855

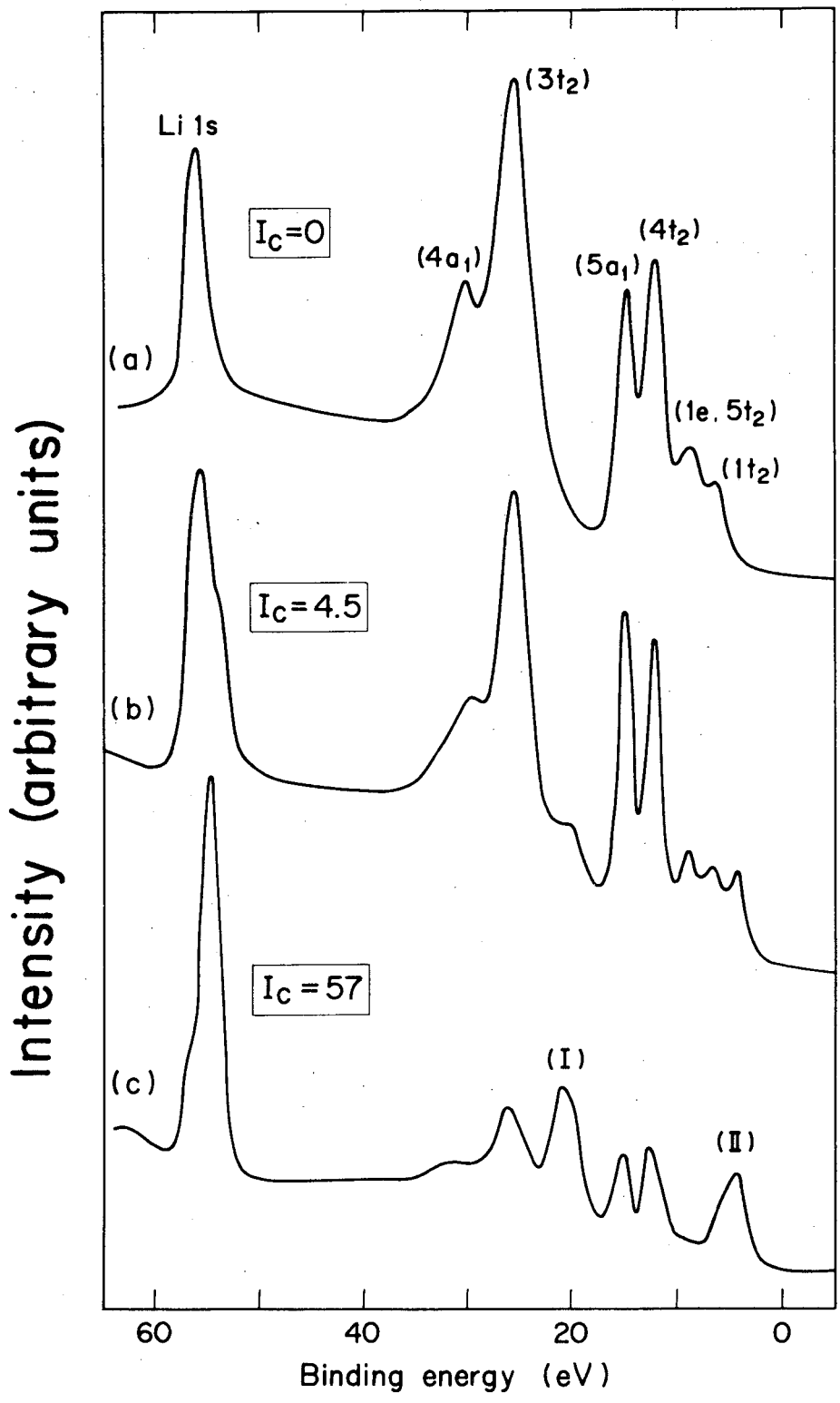


Fig. 7

XBL 7710-6846

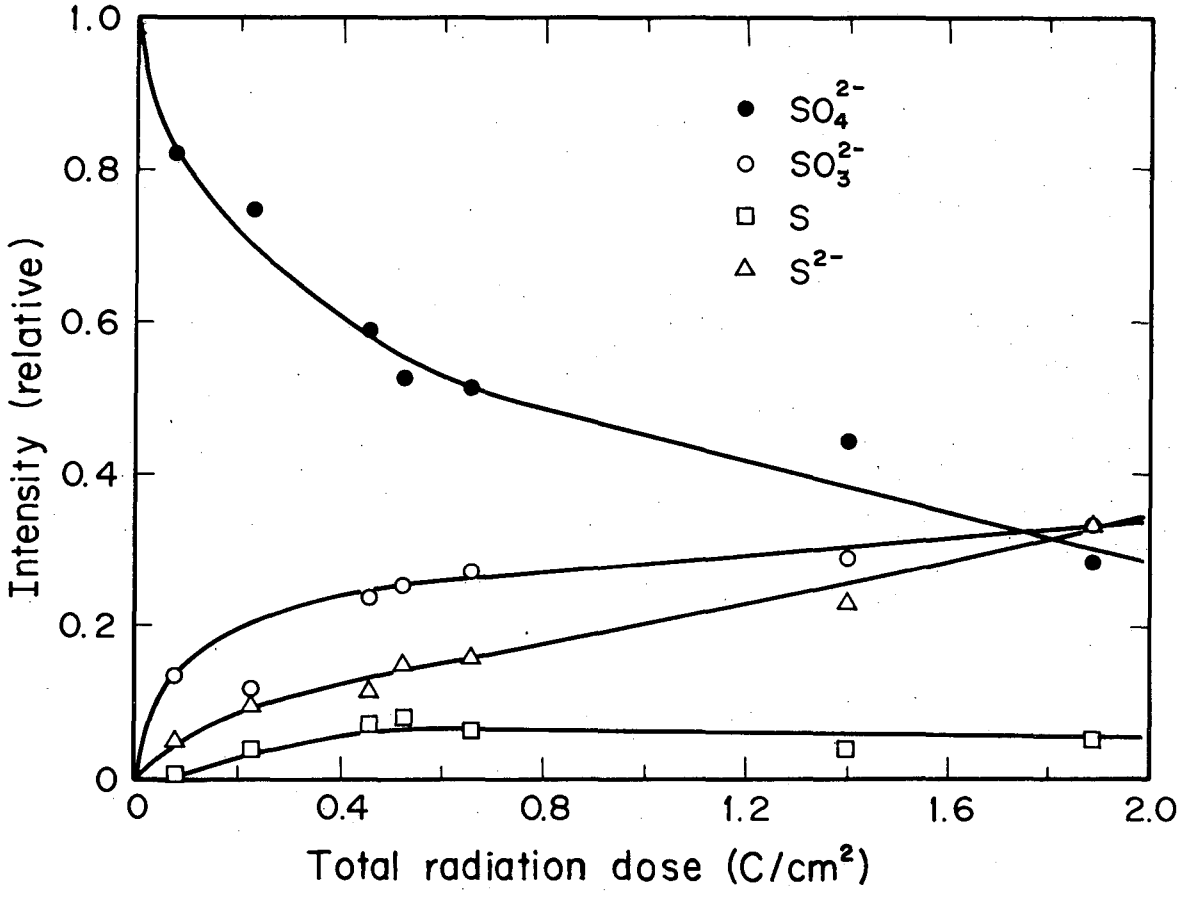


XBL 7710-6854

Fig. 8

0 0 0 0 4 7 1 0 6 1 6



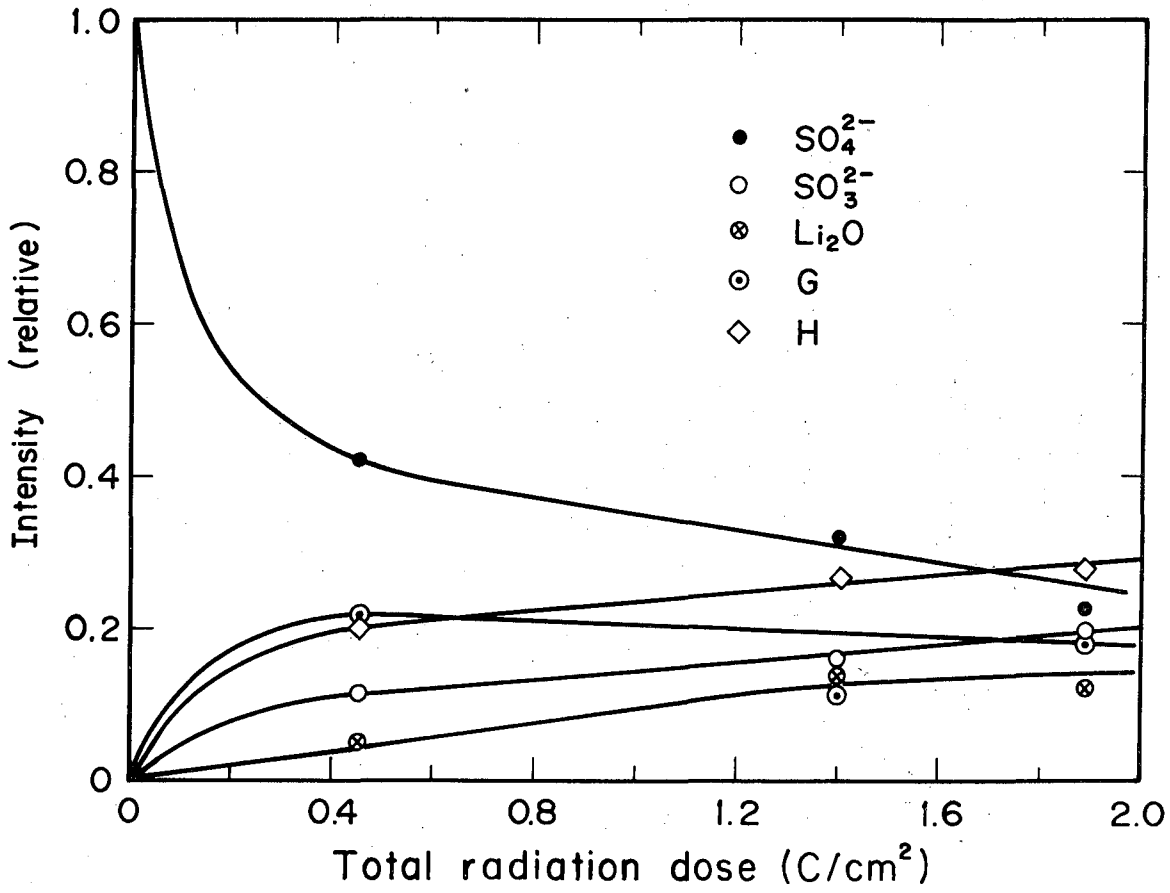


Fig. 9

XBL 7710-6849

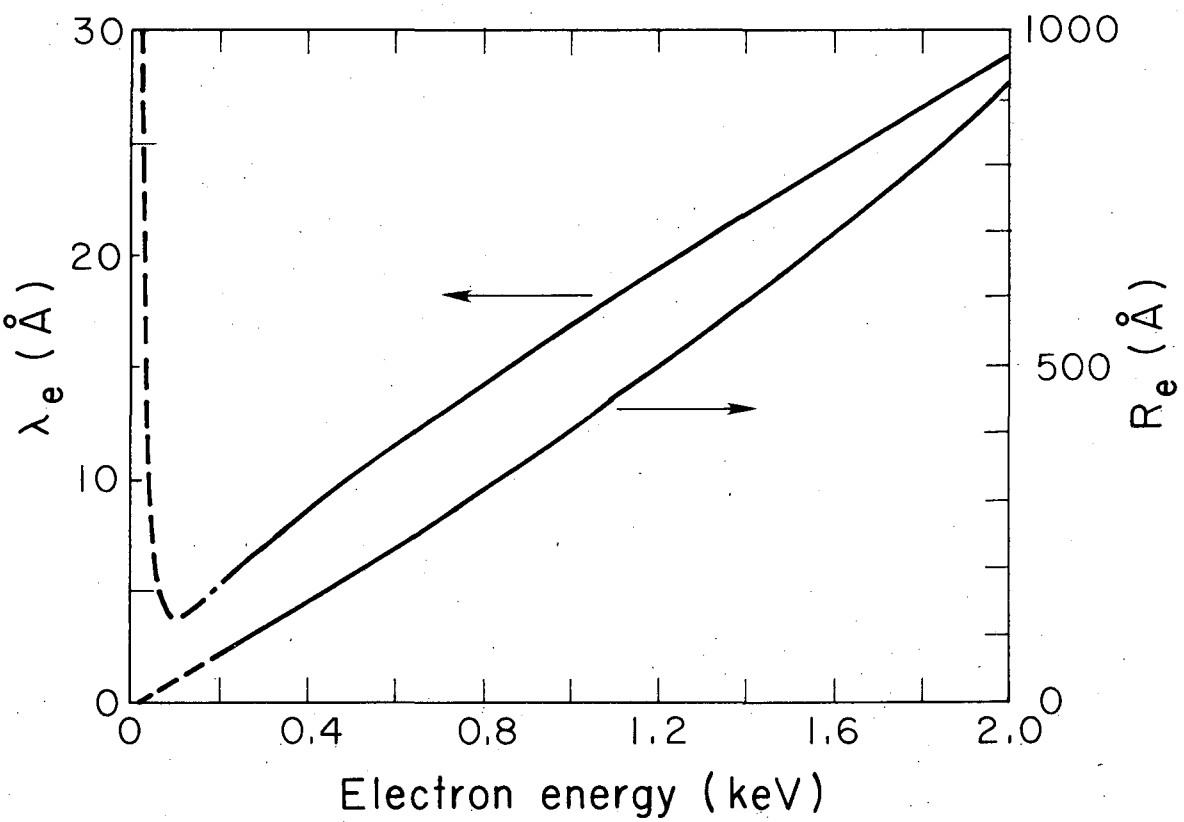


XBL 777-1304

Fig. 10

0 0 0 0 4 7 1 0 6 1 7

This report was done with support from the Department of Energy. Any conclusions or opinions expressed in this report represent solely those of the author(s) and not necessarily those of The Regents of the University of California, the Lawrence Berkeley Laboratory or the Department of Energy.

*TECHNICAL INFORMATION DEPARTMENT*
*LAWRENCE BERKELEY LABORATORY*
*UNIVERSITY OF CALIFORNIA*
*BERKELEY, CALIFORNIA 94720*